Celal Bayar University Journal of Science

Prediction of Antimicrobial Activities of Benzimidazole Derivatives Containing an Amide Bond Through Molecular Docking Analysis

Turgay Tunç¹*

¹Department of Chemistry Engineering, Faculty of Engineering University of Kırşehir Ahi Evran, Kırsehir 40100, Türkiye

* <u>ttunc@ahievran.edu.tr</u> * Orcid No: 0000-0002-2431-8027

Received: December 10, 2024 Accepted: March 20, 2025 DOI: 10.18466/cbayarfbe.1599076

Abstract

Gram-positive and Gram-negative bacterial infections are one of the most important causes of illness and death worldwide. Although antibiotics are the primary treatment for these infections, the increase in the number of drug-resistant bacteria has posed a serious threat to public health in a global scale. Benzimidazole derivatives possess a distinctive chemical structure that exhibits a wide range of biological and therapeutic properties, including notable antimicrobial activity. In this study, we performed molecular docking analyses of four benzimidazole derivatives targeting dihydrofolate reductase, DNA gyrase, and 7,8-dihydro-6-hydroxymethylpterin-pyrophosphokinase enzymes from C. albicans, Escherichia coli, and Staphylococcus aureus. The relative binding free energy of the protein-ligand complexes were also calculated by the molecular mechanics-generalized born surface area (MM-GBSA) method. The relative binding free energy of the protein-ligand complexes were also calculated by the molecular mechanics-generalized born surface area (MM-GBSA) method. All tested compounds showed good potential as dihydrofolate reductase inhibitors and antifungal activity against Candida albicans. Notably, the compound 9A demonstrates the highest antimicrobial activity. Furthermore, all compounds are anticipated to exhibit greater activity against DNA gyrase in both E. coli and S. aureus compared to their respective cognate ligands. Compounds 9A/9B caused higher antimicrobial activity than compounds 10A/10B.

Keywords: Benzimidazole derivatives, amide bonds, molecular docking, antibacterial activity.

1. Introduction

Benzimidazole derivatives are extensively utilized as therapeutic agents for clinical purposes [1-5] because of their significant properties in medicinal chemistry [6-8]. These compounds have become indispensable in drug discovery due to their diverse bioactivities, including anti-protozoal, antimicrobial, anti-inflammatory, analgesic, antioxidant, anthelmintic, antihypertensive, anticancer, anti-human cytomegalovirus, and antiinfluenza properties [9-14]. Additionally, several benzimidazole derivatives have been showed to have antibacterial properties [15-19]. Bacterial infections are among the most prevalent health concerns in both hospital and community environments, contributing significantly to global morbidity and mortality rates. The primary approach to managing these infections involves the use of antibiotics. However, the unnecessary use of antibiotics has led to the emergence of bacterial species or strains resistant to nearly all currently available drugs.

This growing antibiotic resistance crisis is estimated to be responsible for approximately 700,000 deaths annually. Predictions suggest that this number can reach 10 million by 2050 if current trends persist. Although recent antibacterial drugs used in clinical practice are largely modifications of existing antibiotic classes, they offer only temporary effectiveness against specific bacterial species. Consequently, there is an urgent need for the development of novel antibiotics to combat bacterial infections effectively [20]. Four benzimidazole derivatives, illustrated in Figure 1, were synthesized, characterized, and their enzymatic activities were screened in our previous study [21].

Escherichia coli is a gram-negative and rod-shaped bacterium commonly found in the intestines of humans and warm-blooded animals. Most strains of *E. coli* are harmless and play a beneficial role in gut such as helping digestion and vitamin production. However, certain

pathogenic strains of this bacterium can cause severe food-borne diseases, leading to symptoms like diarrhea, abdominal cramps, and in some cases, more severe complications like hemolytic uremic syndrome [22]. Staphylococcus aureus is a gram-positive, spherical (coccus) bacterium that commonly exists as part of the normal skin flora and nasal passages of humans. While many strains of this bacterium are often harmless, it can become pathogenic or opportunistic pathogen under certain conditions and cause different infections such as mild skin and soft tissue infections, boils and impetigo, infections (bacteremia), pneumonia, bloodstream endocarditis, and toxic shock syndrome. S. aureus tends to develop resistance to many different antibiotics. Especially Methicillin-resistant S. aureus (MRSA) is a prominent example, posing challenges in healthcare settings due to its resistance to multiple antibiotics [23]. DNA gyrase subunit B (GyrB) is a critical component of DNA gyrase which is an essential bacterial enzyme introducing negative supercoils into DNA using energy derived from ATP hydrolysis. DNA gyrase, a type II topoisomerase, consists of two subunits: GyrA and GyrB. While GyrA is responsible for DNA cleavage and religation, GyrB provides ATP-binding and hydrolysis activity, which drives the conformational changes necessary for the enzyme's function. GyrB is a key target for antibacterial agents, such as aminocoumarins (e.g., novobiocin) and quinolone antibiotics ciprofloxacin). These drugs inhibit DNA gyrase activity, preventing DNA replication and transcription, ultimately leading to bacterial cell death. Due to its essential role in bacterial survival and its absence in eukaryotic cells, GyrB is a valuable target in the development of novel antibiotics to combat bacterial infections and address antibiotic resistance [24].

In this study, we performed molecular docking analyses of these derivatives against the following enzyme targets: Dihydrofolate reductase (DHFR) from Candida albicans (PDB ID: 1M78), Escherichia coli (PDB IDs: 7NAE and 5U10), and Staphylococcus aureus (PDB ID: 2W9S); DNA gyrase subunit B from Staphylococcus aureus (PDB ID: 3U2D) and Escherichia coli (PDB ID: 1KZN); and 7,8-dihydro-6-hydroxymethylpterin pyrophosphokinase (HPPK) from Staphylococcus aureus (PDB ID: 4CRJ).

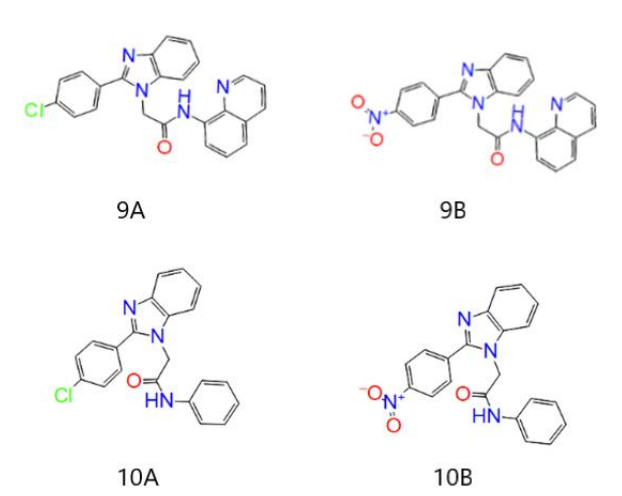


Figure 1. Structure of the compounds.

2. Materials and Methods

2.1. Protein preparation

X-ray crystal structures of the target were imported from the RCSB Protein Data Bank. The enzymes were prepared using the Protein Preparation Wizard module embedded in Schrödinger software (Release, 2020-3). In this process, protein structures were corrected by adding hydrogen atoms and missing residues, assigning bond orders and bond length, creating disulfide bonds, fixing the charges, refining the loop with Prime, removing the water molecules, and finally minimizing by using the OPLS-2005 force field at pH of 7.4. Ionization and tautomeric states were generated by Epik v5.3 and the proton orientations were set by PROPKA. Restrained minimization was run with convergence of heavy atoms to an RMSD of 0.3 Å.

2.2. Ligand preparation

The structure of the compounds which were previously synthesized [21] was optimized at the PM6 level in the water phase using the polarizable continuum solvation method (iefpcm) in Jaguar software. Then, possible ionization and tautomeric states of the compounds were prepared by LigPrep v2.3 module.

2.3. Molecular docking

Schrödinger IFD protocol was used for the IFD-docking calculations [25]. The receptor grid center was specified from the bound cognate ligand with cubic gride. The side chains were automatically trimmed according to the B factor. Default parameters were used for receptor van der Waals scaling factor 0.70 and ligand van der Waals scaling factor 0. All residues within 5.0 Å of ligand poses were refined using the Prime molecular dynamics module to allow for binding domain flexibility. Glide SP protocol with OPLS_2005 force field was used for the redocking step into the top 20 receptor structures

generated within 30 kcal/mol of the best structure by the Prime refinements. The docking method was verified using the redocking test. Cognate ligands were redocked into corresponding binding pockets. RMSD values of the redocked cognate ligands were observed to be in the range of 0.26-0.46 Å, confirming the accuracy and feasibility of the docking method.

2.4. Binding Free Energy Calculations

The relative binding free energy of the protein-ligand the molecular mechanics-generalized born surface area (MM-GBSA) method using the Prime program in Schrodinger software calculated complexes. The OPLS3e force field in the VSGB solvent model was used to calculate energies. The free energy of the complexes was calculated using the equation below.

MMGBSA
$$\triangle G$$
 Bind = $E_{Complex} - E_{Receptor} - E_{Ligand}$

In case of MMGBSA representing molecular mechanics energies combined with the generalized Born and surface area continuum solvation, $\Delta Gbind$ shows the calculated relative free energy of both the ligand and receptor strain energy. Ecomplex represents the MM/GBSA energy of the minimized complex. Ereceptor shows the mean MM/GBSA energy of protein (unbound, minimized) without ligand, and Eligand represents the MM/GBSA energy of the ligand after removing it from the complex [26].

3. Results and Discussion

Target enzymes of microorganisms and their cognate ligands used in molecular docking analysis are listed in Table 1. The IFD docking scores and the best MM-GBSA binding energy values obtained from molecular docking are given in Table 2.

DHFR is a key enzyme in the folic acid pathway and responsible for converting dihydrofolate tetrahydrofolate. This reaction is essential thymidylate biosynthesis, which supports critical cellular processes such as DNA synthesis, RNA transcription, and protein production, ultimately regulating cell growth and proliferation. Various inhibitors of DHFR can effectively disrupt these reactions, making it a valuable target point to control bacterial and fungal growth. That is why, DHFR inhibitors have a great importance for the therapy development against bacterial and fungal infections [27]. The pathogenic yeast Candida albicans exists in various body sites (skin, genital tract, and gastrointestinal tract) of humans as commensal and does not have any harm to the host [28]. The X-ray structure of C. albicans Dihydrofolate Reductase (PDB ID: 1M78) includes 5- Chloryl-2,4,6-quinazolinetriamine (CLZ) as cognate ligand [29]. CLZ (DB01929) is an experimentally small molecule with antifungal properties. IFD docking analysis revealed that the compounds tested in this study showed greater binding

energy than CLZ. Among these, the compound **9A** had the best binding energy (-67.44 kcal/mol). 2D binding interactions and the best docking pose of 9A are shown in Figure 2.

The X-ray structure of *Escherichia coli* K-12 dihydrofolate reductase (PDB ID: 7 NAE) includes trimethoprim (TOP) which is an antifolate antibacterial agent [30]. The X-ray structure of *Escherichia coli* CFT073 dihydrofolate reductase (PDB ID: 5U10) contains pteroic acid (PT1) which is an experimentally small molecule (DB04196) with antibacterial properties [31]. IFD docking analysis revealed that our compounds did not exhibit greater binding energy than the cognate ligands. However, among the tested compounds, **10B** and **9B** showed the best binding energies against *E. coli* K-12 (-77.32 kcal/mol) and *E.coli* CFT073 (-70.12 kcal/mol), respectively.

The X-ray structure of *E. coli* DNA Gyrase (PDB ID: 1 KZN) includes clorobiocin *(CBN)* (an aminocoumarin antibiotic like novobiocin) and coumermycin A1 [32]. IFD docking analysis showed that **9B** exhibited greater binding energy (-74.07 kCal/mol) than the cognate ligand (-67.30 kcal/mol). Its binding interactions and the best docking pose are shown in Figure 3.

The X-ray structure of dihydrofolate reductase (PDB ID: 2W9S), DNA gyrase subunit B (PDB ID: 3U2D) and 7,8-Dihydro-6-hydroxymethylpterin-pyrophosphokinase (HPPK) (PDB ID: 4CRJ) of *S. aureus* contained **trimethoprim** (TOP), 4-bromo-5-methyl-N-[1-(3-nitropyridin-2-yl)piperidin-4-yl]-1H-pyrrole-2-

carboxamide (08B)and 2-amino-8-{[2-(4methoxyphenyl)-2-oxoethyl]sulfanyl}-1,9-dihydro-6Hpurin-6-one (YH5), respectively [33-35]. IFD docking analysis indicated that our compounds did not demonstrate a higher binding energy than trimethoprim as a dihydrofolate reductase inhibitor. However, they showed greater binding energy than the cognate ligand (08B). **9A** demonstrated the best binding energy (70.49 kcal/mol). 2D binding interactions and the best docking pose of 9A are shown in Figure 4. Also, they did not have the higher binding energies than the cognate ligand (YH5) as an HPPK inhibitor. 7,8-Dihydro-6hydroxymethylpterin pyrophosphokinase (HPPK) is an enzyme involved in the biosynthesis of folate (vitamin B9) derivatives, which are crucial for cellular processes such as DNA synthesis and repair.

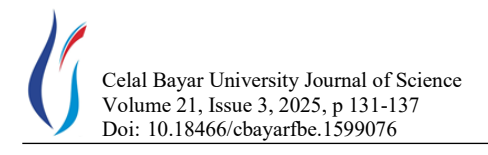


Table 1. The list of microorganisms, target enzymes and their cognate ligands used in this study.

PDB	Microorgani	Target	Cogna
ID	sm		te
1M7	C. albicans	Dihydrofolate	CLZ
8		reductase	
7NA	E. coli K-12	Dihydrofolate	TOP
Е		reductase	
5U1	E.coli	Dihydrofolate	PT1
0	CFT073	reductase	
1KZ	E. coli	DNA gyrase	CBN
N		subunit B	
2W9	S. aureus	Dihydrofolate	TOP
S		reductase	
3U2	S. aureus	DNA gyrase	08B
D		subunit B	
4CR	S. aureus	7,8-Dihydro-6-	YH5
J		hydroxymethylpte	
		rin-	
		pyrophosphokinas	
		e (HPPK)	

Table 2. Docking score (DC) and binding energy (ΔG) of the compounds

	9A	9B	10A	10B	Cognate	
1M78	C. albicans					
DC*	-8.69	-7.94	-8.21	-8.73	-5.06	
ΔG**	-	-	-	-	-22.40	
	67.44	63.56	63.76	55.13		
7NAE	Escheri					
DC	-8.18	-9.76	-	-	-10.09	
			10.81	11.15		
ΔG	-	-	-	-	-88.20	
	64.79	72.17	75.97	77.32		
5U10	Escherichia coli CFT073					
DC	-9.39	-9.55	-7.95	-8.51	-9.93	
ΔG	-	-	-	-	-71.64	
	65.73	70.12	56.37	60.00		
1KZN	Escherichia coli					
DC	-7.01	-7.66	-8.44	-8.20	-7.91	
ΔG	-	-	-	-	-67.30	
	70.91	74.07	69.93	68.35		
2W9S	Staphyl					
DC	-7.43	-7.06	-6.99	-7.33	-9.52	
ΔG	-	-	-	-	-71.43	
	60.90	58.16	60.42	62.96		
3U2D	Staphylococcus aureus					
DC	-7.71	-7.25	-6.85	-6.57	-4.73	
ΔG	-	-	-	-	-52.06	
	70.49	67.02	65.68	55.57		
4CRJ	Staphyl					
DC	-5.02	-5.02	-6.27	-4.52	-10.52	
ΔG	-	-	-	-	-83.08	
	44.21	50.15	41.73	33.77		

*IFD Binding Score(kcal/mol), **MM-GBSA binding energy (kcal/mol)

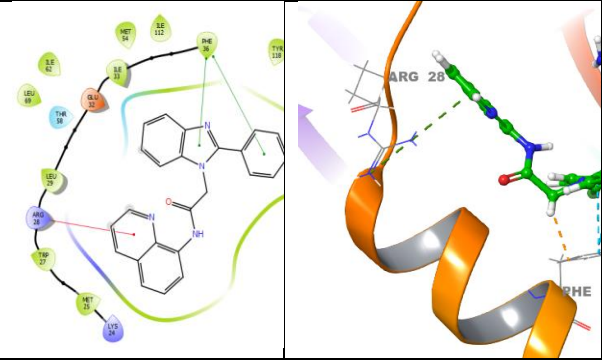


Figure 2. 2D binding interaction (left) and 3D binding diagram of **9A** in Candida albicans DHFR (PDB ID: 1M78)

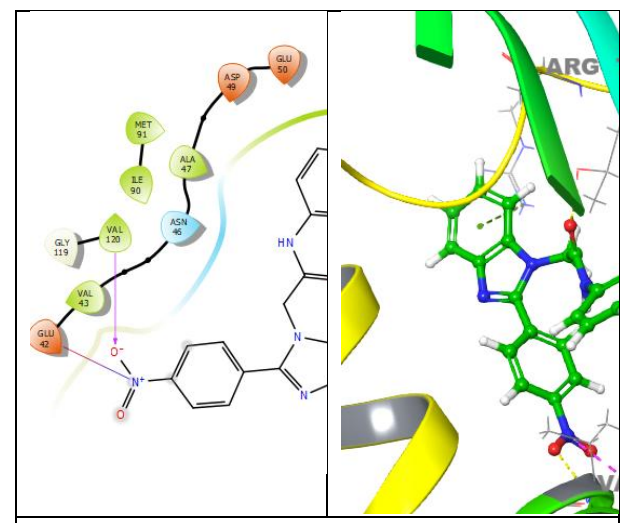


Figure 3. 2D binding interaction (left) and 3D binding diagram of **9B** in *E. coli* DNA Gyrase (PDB ID: 1 KZN)

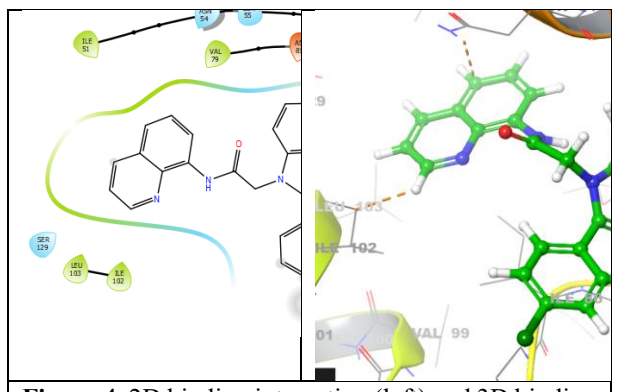


Figure 4. 2D binding interaction (left) and 3D binding diagram of **9A** in *S.Aureus* DNA Gyrase (PDB ID: 3U2D)

Based on IFD docking analysis and MMGBSA ΔG binding energy calculations, we were able to make predictions for the behavior of the compounds tested in this study:

All compounds have the potential to function as dihydrofolate reductase inhibitors, with predicted

antifungal activity against *C. albicans*. Among them, 9A exhibited the strongest activity. The binding energy of 9A (-67.44 kcal/mol) was significantly more negative compared to the cognate ligand (-22.40 kcal/mol).

All compounds showed potential activity against *E. coli* dihydrofolate reductase enzyme. However, none of them had stronger antifolate activity against *E. coli* DHFR compared to trimethoprim (TOP). Notably, 9B (binding energy: -70.12 kcal/mol) shows activity comparable to pteroic acid (binding energy: -71.64 kcal/mol). Additionally, all compounds were predicted to exhibit stronger activity against *E. coli* DNA gyrase than the cognate ligand clorobiocin (CBN).

4. Conclusion

None of the compounds were expected to show stronger antifolate activity against *S. aureus* DHFR compared to trimethoprim (TOP). However, all of them were predicted to show greater activity against *S. aureus* DNA gyrase than the cognate 4-bromo-5-methyl-N-[1-(3-nitropyridin-2-yl)piperidin-4-yl]-1H-pyrrole-2-carboxamide (08B). In contrast, all produced only half the activity against *S. aureus* 7,8-dihydro-6-hydroxymethylpterin pyrophosphokinase (HPPK) compared to the cognate ligand YH5. Compounds 9A/9B were likely to cause greater activity compared to compounds 10A/10B.

Acknowledgement

The research was financially supported by Kirsehir Ahi Evran University BAP unit (grant no. MMF.A4.22.017).

Author's Contributions

Turgay Tunç: Performed all experiments and data analysis. Wrote and revised the manuscript.

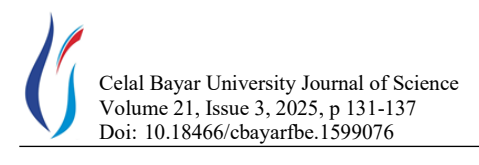
Ethics

There are no ethical issues after the publication of this manuscript.

References

- [1]. Preston, PN. 1974. Synthesis, reactions, and spectroscopic properties of benzimidazoles. *Chem. Rev*; 74: 279–314.
- [2]. Sundberg, RJ, Martin, RB. 1974. Interactions of histidine and other imidazole derivatives with transition metal ions in chemical and biological systems. *Chem. Rev*; 74: 471–517.
- [3]. Nájera, C, Yus, M. 2015. Chiral benzimidazoles as hydrogen bonding organocatalysts. *Tetrahedron Lett*; 56: 2623–2633. [4]. Khose, VN, John ME, Pandey AD, Karnik, AV. 2017. Chiral benziimidazoles and their applications in stereodiscrimination processes. *Tetrahedron Asymmetry*; 28: 1233–1289.
- [5]. Asensio, JA, Sanchez, EM, Gómez-Romero, P. 2010. Proton-conducting membranes based on benzimidazolepolymers for high-

- temperature PEMfuelcells. A chemical quest. *Chem. Soc. Rev*; 39: 3210–3239.
- [6]. Al-Muhaimeed, HS. 1997. A parallel-group comparison of Astemizole and Loratadine for the treatment of perennial allergic rhinitis. *J. Int. Med. Res*; 25: 175–181.
- [7]. Scott, LJ, Dunn, CJ, Mallarkey G, Sharpe, M. 2002. Esomeprazole: a review of its use in the management of acid-related disorders. *Drugs*; 62: 1503–1538.
- [8]. Gaba, M, Singh, S, Mohan, C. 2014. Benzimidazole: an emerging scaffold for analgesic and anti-inflammatory agents. *Eur. J. Med. Chem*: 76: 494–505.
- [9]. Horton, DA, Bourne, GT, Sinythe, ML. 2003. The combinatorial synthesis of bicyclic privileged structures or privileged substructures. *Chem. Rev*; 103: 893–930.
- [10]. Alamgir, M, Black, DSC, Kumar, N. 2007. Synthesis, reactivity and biological activity of Benzimidazoles. *Heterocycl. Chem*; 9: 87–118
- [11]. Goker, H, Ozden, S, Yildiz, S, Boykin, DW. 2005. Synthesis and potent antibacterial activity against MRSA of some novel 1,2-disubstituted-1H-benzimidazole-N-alkylated-5-carboxamidines. *Eur. J. Med. Chem*; 40: 1062–1069.
- [12]. Abraham, R, Periakaruppan, P, Mahendran, K, Ramanathan, M. 2018. A novel series of N-acyl substituted indole-linked benzimidazoles and naphthoimidazoles as potential antiinflammatory, anti-biofilm and anti-microbial agents. *Microb. Pathog*; 114: 409–413.
- [13]. Zhu, Z, Lippa, B, Drach, DJ, Townsend, LB. 2000. Design, synthesis, and biological evaluation of tricyclic nucleosides (dimensional probes) as analogues of certain antiviral polyhalogenated benzimidazole ribonucleosides. *J. Med. Chem*; 43: 2430–2437.
- [14]. Mann, J, Baron, A, Opoku-Boahen, Y, Johansson, E, Parkinson, G, Kelland, LR, Neidle, S. 2001. A new class of symmetric bisbenzimidazole-based DNA minör groove-binding agents showing antitumor activity. *J. Med. Chem*; 44: 138–144.
- [15]. Sambanthamoorthy, K, Gokhale, AA, Lao, W, Parashar, V, Neiditch, MB, Semmelhack, MF, Lee, I, Waters, CM. 2011. Identification of a novel benzimidazole that inhibits bacterial biofilm formation in a broad-spectrum manner. *Antimicrob. Agents Chemother*; 55: 4369–4378.
- [16]. Singu, PS, Kanugal, S, Dhawale, SA, Kumar, CG, Ravindra, M, Kumbhare, RM. 2020. Synthesis and pharmacological evaluation of some amide functionalized 1H-Benzo[d]imidazole-2-thiol derivatives as anti-microbial agents. *Chemistry Select*; 5: 117–123.
- [17]. Reddy, NB, Grigory, V, Zyryanov, GV, Reddy GM, Balakrishna, A, Padmaja A, Padmavathi, V, Reddy, CS, Garcia, JR, Sravya, G. 2019. Design and synthesis of some new benzimidazole containing pyrazoles and pyrazolyl thiazoles as potential anti-microbial agents. *J. Heterocycl. Chem*; 56: 589–596.
- [18]. Shi, Y, Jiang, K, Zheng, R, Fu, J, Yan, L, Gu, Q, Zhang, Y, Lin, F. 2019. Design, microwave-assisted synthesis and in vitro antibacterial and antifungal activity of 2,5-disubstituted benzimidazole. *Chem. Biodivers*; 16: e1800510.
- [19]. Obaiah, N, Bodke ND, Telkar, S. 2020. Synthesis of 3-[(1H-Benzimidazol-2-ylsulfanyl)(aryl)methyl]-4-hydroxycoumarin derivatives as potent bioactive molecules, *Chemistry Select*; 5: 178–184.
- [20]. Feng, D, Zhang, A, Yang, Y, Yang, P. 2020. Coumarin-containing hybrids and their antibacterial activities. *Archiv Der Pharmazie*; 353(6): 1900380.



- [21]. Alım, Z, Tunç, T, Demirel, N, Günel, A, Karacan, N. 2022. Synthesis of benzimidazole derivatives containing amide bond and biological evaluation as acetylcholinesterase, carbonic anhydrase I and II inhibitors. *Journal of Molecular Structure*; 1268: 133647.
- [22]. Basavaraju, M, Gunashree, BS. 2022. Escherichia coli: an overview of main characteristics. *Escherichia coli-Old and New Insights*.
- [23]. Peacock, S, 2006. Staphylococcus aureus. *Principles and practice of clinical bacteriology*, 2, 73-98.
- [24]. Reece, RJ, Maxwell, A. 1991. DNA gyrase: structure and function. *Critical reviews in biochemistry and molecular biology*, 26 (3-4), 335-375.
- [25]. Nabuurs, SB, Wagener, M, De Vlieg, J. 2007. A Flexible approach to induced fit docking. *Journal of Medicinal Chemistry*; 50(26): 6507–6518
- [26]. Genheden, S, Ryde, U. 2015. The MM/PBSA and MM/GBSA methods to estimate ligand-binding affinities. *Expert Opinion on Drug Discovery*; 10(5): 449–461.
- [27]. Shahabadi, N, Mahdavi, M. 2023. Green synthesized silver nanoparticles obtained from Stachys schtschegleevii extract: Ct-DNA interaction and *in silico* and *in vitro* investigation of antimicrobial activity. *Journal of Biomolecular Structure and Dynamics*; 41(6): 2175–2188.
- [28]. Costa-de-Oliveira, S, Rodrigues, AG. 2020. Candida albicans antifungal resistance and tolerance in bloodstream infections: the triad yeast-host-antifungal. *Microorganisms*; 8(2): 154-173.
- [29]. Whitlow, M, Howard, AJ, Stewart, D, Hardman, KD, Kuyper, LF, Baccanari, DP, Fling, ME, Tansik, RL. 1997. X-ray crystallographic studies of candida albicans dihydrofolate reductase. *Journal of Biological Chemistry*; 272(48): 30289–30298.
- [30]. Krucinska, J, Lombardo, MN, Erlandsen, H, Estrada, A, Si, D, Viswanathan, K, Wright, DL. 2022. Structure-guided functional studies of plasmidencoded dihydrofolate reductases reveal a common mechanism of trimethoprim resistance in Gram-negative pathogens. *Communications Biology*; 5: 459.
- [31]. Dennis, ML, Lee, MD, Harjani, JR, Ahmed, M, DeBono, AJ, Pitcher, NP, Wang, Z, Chhabra, S, Barlow, N, Rahmani, R, Cleary, B,

- Dolezal, O, Hattarki, M, Aurelio, L, Shonberg, J, Graham, B, Peat, TS, Baell, JB, Swarbrick, JD. 2018. 8-Mercaptoguanine derivatives as inhibitors of dihydropteroate synthase. *Chemistry A European Journal*; 24(8): 1922–1930.
- [32]. Lafitte, D, Lamour, V, Tsvetkov, PO, Makarov, AA, Klich, M, Deprez, P, Moras, D, Briand, C, Gilli, R. 2002. Dna gyrase interaction with coumarin-based inhibitors: the role of the hydroxybenzoate isopentenyl moiety and the 5'-methyl group of the noviose. *Biochemistry*; 41(23): 7217–7223.
- [33]. Dennis, ML, Chhabra, S, Wang, ZC, Debono, A, Dolezal, O, Newman, J, Pitcher, NP, Rahmani, R, Cleary, B, Barlow, N, Hattarki, M, Graham, B, Peat, TS, Baell, JB, Swarbrick, JD. 2014. Structure-based design and development of functionalized mercaptoguanine derivatives as inhibitors of the folate biosynthesis pathway enzyme 6-hydroxymethyl-7,8-dihydropterin pyrophosphokinase from staphylococcus aureus. Journal of Medicinal Chemistry; 57(22): 9612–9626.
- [34]. Eakin, AE, Green, O, Hales, N, Walkup, GK, Bist, S, Singh, A, Mullen, G, Bryant, J, Embrey, K, Gao, N, Breeze, A, Timms, D, Andrews, B, Uria-Nickelsen, M, Demeritt, J, Loch, JT, Hull, K, Blodgett, A, Illingworth, RN, Sherer, B. 2012. Pyrrolamide dna gyrase inhibitors: fragment-based nuclear magnetic resonance screening to identify antibacterial agents. *Antimicrobial Agents and Chemotherapy*; 56(3): 1240–1246.
- [35]. Heaslet, H, Harris, M, Fahnoe, K, Sarver, R, Putz, H, Chang, J, Subramanyam, C, Barreiro, G, Miller, JR. 2009. Structural comparison of chromosomal and exogenous dihydrofolate reductase from *Staphylococcus aureus* in complex with the potent inhibitor trimethoprim. *Proteins: Structure, Function, and Bioinformatics*; 76(3): 706–717